2026 IEEE International Conference on Robotics and Automation (ICRA 2026)
June 1-5, 2026. Vienna, Austria

A Gripper with Extreme Stiffness Anisotropy for High-Speed Handling of Fragile Foods

Zhongkui Wang[1], Mutsuhito Sato[2], Mengyao Liu[1], Hikaru Arita[3], Yoshiki Mori[4], and Sadao Kawamura[5]

***Abstract*— Handling fragile objects at high speeds presents a significant challenge. To address this challenge, researchers explored hybrid grippers and grippers with adjustable stiffness. However, grippers exhibiting anisotropic stiffness have received little attention. This paper presents an extreme case of an anisotropic stiffness gripper designed for high-speed handling of delicate foods. The proposed gripper incorporates linear motors and low-friction linear guides. Its extremely low friction in the grasping direction ensures minimal grasping force (less than 0.1 N) and high compliance, enabling the secure handling of fragile objects. Simultaneously, its rigid structure provides sufficient stiffness in the translational direction, ensuring stability during high-speed motion. Leveraging anisotropic stiffness, the gripper achieves both gentle grasp and stable high-speed translation—two requirements that typically necessitate a trade-off. Theoretical analysis was conducted to determine the maximum permissible acceleration under two conditions: with and without stiffness anisotropy. Results indicate that stiffness anisotropy enables significantly higher acceleration during translational motion, thereby reducing task time. Pick-and-place experiments on a 3D printed object, delicate foods of a potato chip, a block of tofu, and a piece of dried seaweed validated theoretical findings and demonstrated the gripper's capability to handle fragile objects at high speeds effectively.**

I. Introduction

In recent years, the manufacturing industry has faced labor shortages due to an aging population and declining birth rate. The food industry, in particular, remains less automated compared to sectors such as automotive and electronics [1]. Automating food production lines offers multiple benefits, such as reducing labor costs, minimizing the risk of contamination, and improving overall productivity [2]. Additionally, fully automated production lines can help maintain a closed cold chain from production to consumption, potentially extending product shelf life and reducing food waste [3]. However, several challenges must be addressed to facilitate automation in the food industry, including the absence of suitable robotic end-effectors, difficulties in food recognition, and a lack of fundamental data on food properties [4]. Among these challenges, the development of robotic end-effectors capable of handling diverse food products remains the most significant barrier to the widespread adoption of robotic systems in food production. This challenge becomes particularly critical when considering the high-speed handling of fragile food products such as tofu, raw oysters, and potato chip, for which very few grippers exist.

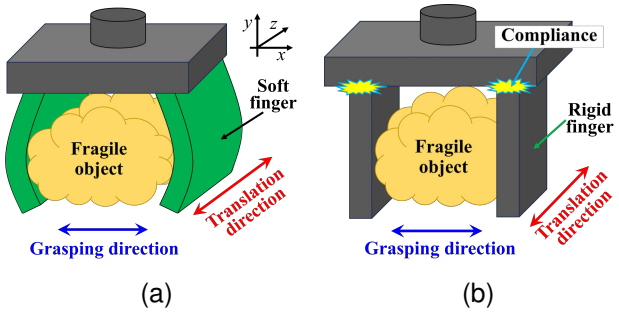

Fig. 1. Stiffness anisotropy in (a) soft gripper and (b) rigid gripper.

For handling flexible and deformable object, a variety of robotic end-effectors have been developed. Among these, suction cups are the most widely studied and used in the industry for high-speed handling operations [5]. Suction cups have many advantages, such as simple structure, low cost, and less footprint on object surface, but they usually require the object surface to be relatively flat, smooth, dry, and airtight. To overcome these limitations and handle porous and flexible objects, such as textile materials, Bernoulli gripper [6] and vortex gripper [7] were developed using outward air flow to generate vacuum pressure for grasping, which can realize low-contact or non-contact grasping.

For handling fragile objects, two strategies were often adopted when designing a gripper. One is to use force control based on sensor feedback and the other is to purely use passive compliance or flexibility within the gripper body to reduce damage upon contact. To realize distributed force feedback, flexible tactile sensors were usually used such as the one proposed in [8] and commercially available FlexiForce sensors [9]. In addition, force sensing based on air pressure in a pre-inflated chamber [10] and Permanent Magnet Elastomer (PME) membrane [11] were also proposed for grasping cherry tomato, egg, banana, and roll cake. Without relying on sensory data, researchers focused on gripper ideas capable of generating as large contact area as possible to minimize the damage on fragile objects, such as the ROSE gripper [12], the soft enveloping gripper [13], gripper with shape-adaptive skin [14], the gripper with incompressible fluid-based deformable fingertips [15], and the gripper with fin ray structure [16]. They have been successfully utilized

This work was supported by JSPS KAKENHI Grant Number JP24K00856.

[1]Zhongkui Wang and Mengyao Liu are with the Department of Robotics, Ritsumeikan University, Kusatsu, Shiga 525-8577, Japan wangzk@fc.ritsumei.ac.jp

[2]Mutsuhito Sato is with Toyota Motor Corporation, Toyota, Aichi, Japan

[3]Hikaru Arita is with the Department of Mechanical Engineering, Kyushu University, Fukuoka, Japan arita@mech.kyushu-u.ac.jp

[4]Yoshiki Mori is with the School/Graduate School of Engineering Science, The University of Osaka, Osaka, Japan

[5]Sadao Kawamura is with Ritsumeikan Global Innovation Research Organization, Ritsumeikan University, Kusatsu, Japan

for handling fragile objects, such as jelly, grape, tofu, potato chips, and tomato. However, handling operations under high-speed motions were not addressed sufficiently.

When handling fragile object under high-speed motions, inertial force plays an important role and large acceleration may damage the object [17]. In such scenario, trade-off between gripper compliance and stiffness must be made for reducing object damage but still realizing stabile handling under high acceleration. To address this challenge, researchers proposed grippers with variable stiffness and soft-rigid hybrid structures. Jamming effect is the most widely used approach to realize stiffness adjustment. Researchers have investigated granular jamming [18] and layer jamming [19] for various applications. Jamming grippers can realize stiffness transition upon actuation and can handle various shaped objects. However, the stiffness transition requires time for gripping (0.1 s∼0.7 s) and releasing (0.15 s∼1 s) [20], which may limit their applications for high frequent handling. Grippers with soft-rigid hybrid structures often involve soft chamber with rigid backbone [21], [22] or soft strings with rigid frame [23], [24] for taking advantages of both soft and rigid materials.

Another way to address this trade-off between low stiffness for grasping and high stiffness for translation is to utilize the stiffness anisotropy of the gripper during different motions. This approach can be effective when considered together with gripper compliance, but unfortunately it has not been investigated frequently. Yang *et al.* developed a trap-like soft gripper with multiple tentacle fingers, utilizing stiffness anisotropy to create a "trap" mechanism that allows the target to enter easily but prevents it from escaping [25]. Similarly, Assenbergh *et al.* introduced anisotropic soft pads for a surgical gripper, enabling a secure yet gentle grip on delicate tissues [26]. Mykhailyshyn *et al.* revealed that gripping performances of textile objects using pneumatic grippers can be improved by adjusting the orientation and position of the gripper during lifting motion [27]. While these studies successfully applied gripper anisotropy to improve grasping performances, object handling under high-speed motion has not been sufficiently addressed.

To this end, this paper presents an extreme case of a gripper capable of achieving both highly compliant grasping and high-speed translation by using stiffness anisotropy. The key contributions of this paper are:

- A robotic gripper with extreme stiffness anisotropy was proposed for handling fragile foods. The minimum grasping force was experimentally characterized to be less than 0.1 N, providing sufficient compliance for delicate grasping;
- Theoretical analysis was conducted to determine the maximum acceleration for pick-and-place motions, with and without the use of stiffness anisotropy. The results were validated by experiments;
- High-speed pick-and-place experiments on various fragile food items were conducted to evaluate the performance of the proposed gripper and the handling strategy of using stiffness anisotropy.

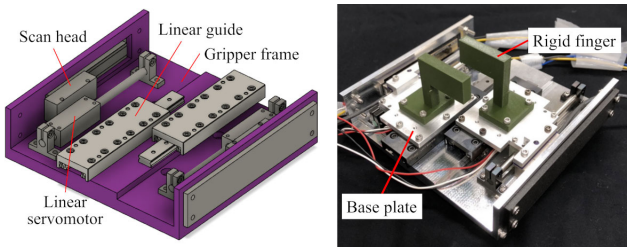

Fig. 2. Gripper design (a) and the fabricated gripper (b).

II. Anisotropic Gripper

A. Stiffness Anisotropy

When grasping fragile objects with robotic grippers, many researchers have employed soft fingers to minimize impact and prevent damage, as illustrated in Fig. 1a. Soft fingers provide compliance and flexibility in the grasping direction, allowing them to conform to the object's geometry and reduce stress. However, this compliance also leads to excessive vibrations or shaking during high-speed motion, which can result in handling failures [17].

To enhance high-speed performance, one straightforward approach is to leverage stiffness anisotropy by ensuring higher finger stiffness in the direction of high-speed translation. This can be achieved by increasing the width of the soft fingers. However, when fabricated entirely from soft materials, the achievable stiffness anisotropy remains limited. Therefore, we explore an extreme case of stiffness anisotropy using rigid fingers, as depicted in Fig. 1b.

High compliance in the grasping direction is achieved through the integration of linear motors and low-friction guide rails. Without relying on force sensors, force control is realized, enabling the gripper to exert a minimal grasping force of less than 0.1 N, which is significantly lower than that of most pneumatic soft grippers. In the translation direction, the rigid fingers exhibit no compliance and can be considered having infinite stiffness, effectively eliminating vibrations and shaking during high-speed handling.

B. Gripper Design and Manufacture

To implement the concept illustrated in Fig. 1b, a parallel gripper was developed using a linear servomotor (SX060T-60st-L126-10L2, Nippon Pulse Motor) and a low-friction linear guide (VRT2095, THK) [28]. The linear servomotor, also known as a shaft motor, operates with minimal friction since it does not require a reduction gear. The gripper design is shown in Fig. 2a. It consists of two linear servomotors and two linear guides, enabling independent control.

To actuate the servomotors, scan heads are required and are mounted adjacent to the motors. Since using a linear motor alone can introduce undesired rotational motion, a linear guide is employed to constrain movement and establish a direct connection between the motor and the finger. The guide rail consists of a table and a rail, where natural friction occurs. To minimize this friction, the low-friction guide rail

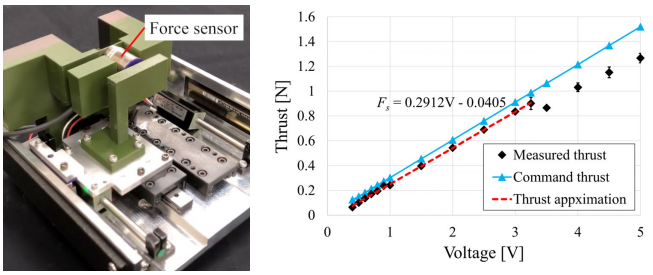

Fig. 3. Grasping force calibration: (a) experimental setup and (b) calibration results.

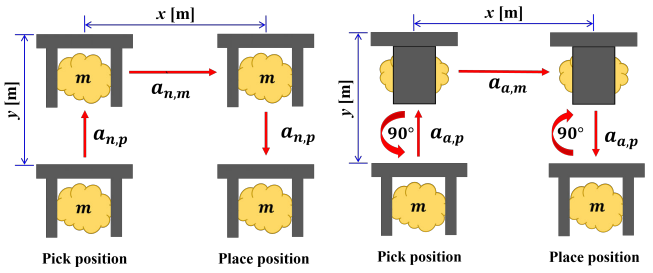

Fig. 4. Pick-and-place motions: (a) without using stiffness ansiotropy (analyzed by the pick-up acceleration $a_{n,p}$ and translation acceleration $a_{n,m}$) and (b) with using stiffness anisotropy (analyzed by the pick-up acceleration $a_{a,p}$ and translation acceleration $a_{a,m}$).

(VRT2095, THK) was selected. The manufactured gripper is shown in Fig. 2b.

To ensure high assembly accuracy, the gripper frame and base plate—responsible for connecting the motor and guide rail—were precision-machined from stainless steel. The two rigid fingers were 3D printed using PLA material and mounted onto the base plate, forming a parallel gripper structure. Force control is achieved by adjusting input voltages through a motor driver (MADLT11SM, Panasonic) and a microcontroller (Arduino Uno) [28]. The overall dimensions of the gripper are 173 mm×160 mm×87.7 mm, with a total mass of 1.8 kg.

C. Gripper Characterization

To calibrate the grasping force, a 6-axis force sensor (PFS020YA500U6, Leptrino) was mounted on a frame fixed to the gripper's base plate, as shown in Fig. 3a. Various input voltages were applied to the linear motor to press the finger against the force sensor, and the corresponding forces were recorded. The measured forces are presented in Fig. 3b. A sudden drop in the measured force was observed at voltages around 3.25 V, which was attributed to misalignment along the assembly axis. Since this study primarily focuses on sub-Newton-level forces, only the experimental data collected before 3.25 V was considered for analysis. The selected data was subsequently fitted using the following linear equation.

$$F_s = 0.2912V - 0.0405$$

where F_s and V denote the thrust force (N) and applied voltage (V), respectively. Since the minimum force required for stable finger movement occurs at a voltage of 0.4 V, the minimum grasping force can be determined by substituting V = 0.4 V into the equation. Consequently, the minimum grasping force is characterized as approximately 0.076 N, which is sufficiently small for handling various fragile food items. Additionally, as shown in Fig. 3, discrepancies between the commanded and measured thrust forces are observed. These differences are attributed to the static friction present in the linear guide.

III. Theoretical Analysis

A. Problem Definition

We conduct the motion analysis by defining a typical pick-and-place task, as illustrated in Fig. 4. When the task is performed without utilizing stiffness anisotropy (Fig. 4a), the required motions include the followings:

1) Grasping the object at the pick position.
2) Lifting the object to a height of y meters.
3) Translating the object over a distance of x meters.
4) Lowering the object with a same height of y meters.
5) Placing the object at the target position.

Throughout these motions, the orientation of the gripper remains unchanged.

On the other hand, when stiffness anisotropy is utilized, a rotational motion is introduced during the lifting and lowering phases, as illustrated in Fig. 4b, to adjust the gripper's orientation. By rotating the gripper by 90 degrees, high stiffness can be achieved during high-speed translation, which is expected to enhance performance by enabling higher operational speeds. To validate this hypothesis, the following sections present a theoretical analysis of the maximum allowable accelerations and the required time to successfully complete the pick-and-place task for both cases—without and with using stiffness anisotropy.

As discussed above, the pick-and-place motion can be divided into three distinct phases: lifting, translation, and lowering. Each of these motions can be modeled as a linear movement consisting of an acceleration phase followed by a deceleration phase. To achieve high-speed pick-and-place operations, we assume that the robot moves at its maximum allowable acceleration. However, due to the relatively short translation distances x and y, the robot typically does not reach its maximum velocity. Consequently, in the following analysis, we model the robot's velocity using a triangular profile, as illustrated in Fig. 5a. The experimentally measured velocity profile, obtained using a 6-DOF robotic manipulator (Melfa RV-4FRL-D, Mitsubishi Electric Corp.), is shown in Fig. 5b. Under the triangular velocity profile, the relationships between the translation distance x, maximum velocity v_{max}, maximum acceleration a_{max}, and task time t are expressed as follows.

$$x = v_{max}t/2, \tag{1a}$$

$$v_{max} = a_{max}t/2, \tag{1b}$$

$$t = 2\sqrt{x/a_{max}}. \tag{1c}$$

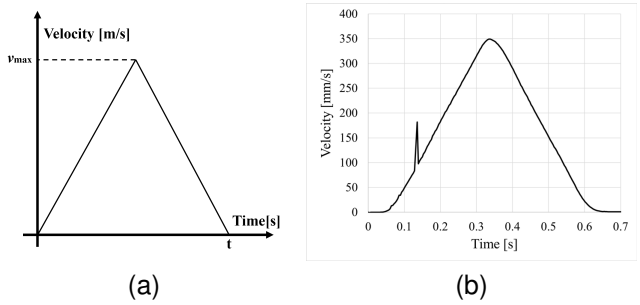

Fig. 5. Velocity profiles of (a) designed and (b) measured curves.

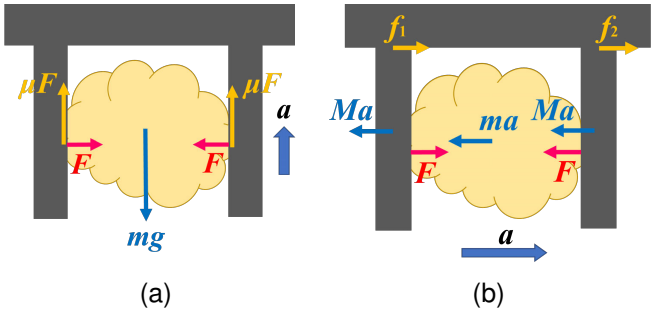

Fig. 6. Force analysis during (a) the pick-up motion and (b) the translation motion in the scenario without using stiffness anisotropy.

B. Motion Analysis without Stiffness Anisotropy

As discussed above, the task time is dependent on the maximum allowable acceleration (Eq. 1c). To determine the maximum allowable accelerations for different motion phases, we first consider the pick-up motion of the food, as illustrated in Fig. 6a. The equation of motion in the vertical direction can be derived as follows:

$$2\mu F - mg \geq ma, \tag{2}$$

where μ, F, m, g, and a represent the friction coefficient between the gripper and the food, the grasping force, the mass of the food, the gravitational acceleration, and the robot acceleration during the pick-up motion, respectively. The maximum acceleration $a_{n,p}$ can be then calculated as follows:

$$a_{n,p} = 2\mu F/m - g. \tag{3}$$

Secondly, when analyzing the translation motion of the two fingers and the food, as illustrated in Fig. 6b, the equation of motion in the horizontal direction can be derived as follows:

$$f_1 + f_2 \geq (2M+m)a, \tag{4}$$

where M indicates the mass of one finger; f_1 and f_2 represent the back-drive force of each finger, respectively. The total back-drive force, (f_1+f_2), was calibrated as 0.122N [28]. To account for uncertainties in the back-drive force, a safety factor S is introduced into the equation. The maximum acceleration $a_{n,m}$ can then be calculated as follows:

$$a_{n,m} = \frac{f_1+f_2}{(2M+m)S}, \tag{5}$$

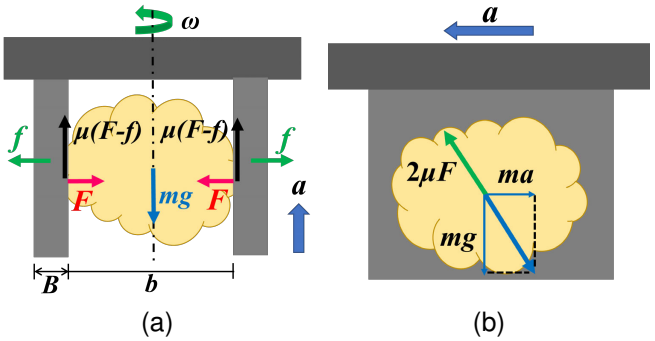

Fig. 7. Force analysis during (a) the pick-up motion and (b) the translation motion in the scenario with using stiffness anisotropy.

Finally, by substituting Eqs. 3 and 5 into Eq. 1c, the total time t_n required to complete the pick-and-place motion without stiffness anisotropy can be determined as follows:

$$\begin{aligned} t_n &= 4\sqrt{\frac{y}{a_{n,p}}} + 2\sqrt{\frac{x}{a_{n,m}}} \\ &= 4\sqrt{\frac{my}{2\mu F - mg}} + 2\sqrt{\frac{xS(2M+m)}{f_1+f_2}}. \end{aligned} \tag{6}$$

C. Motion Analysis with Stiffness Anisotropy

When stiffness anisotropy is utilized, the gripper must rotate 90 degrees during the lifting motion. Considering the lifting motion accompanied by rotation, as illustrated in Fig. 7a, both fingers experience a centrifugal force f which can be calculated as

$$f = M\omega^2(B+b)/2, \tag{7}$$

where ω, B, and b represent the angular velocity, the width of the finger, and the width of the food, respectively. The force balance in the vertical direction yields the following equation:

$$2\mu(F-f) - mg \geq ma. \tag{8}$$

If the rotation and lifting motions conclude simultaneously, the following relationships hold:

$$\omega t = \theta, \qquad t = 2\sqrt{y/a}. \tag{9}$$

where θ represents the rotation angle in radians.

By solving Eqs. 7, 8, 9, the maximum allowable acceleration can be determined as follows:

$$a_{a,p} = \frac{4y(2\mu F - mg)}{4ym + \mu M\theta^2(B+b)}. \tag{10}$$

On the other hand, when analyzing the translation motion with stiffness isotropy, the force analysis in the non-inertial reference frame (attached to the gripper) is illustrated in Fig. 7b. The force balance equation can then be expressed as follows:

$$m\sqrt{a^2+g^2} \leq 2\mu F. \tag{11}$$

Then, the maximum allowable acceleration during translation can be calculated as follows:

$$a_{a,m} = \frac{\sqrt{4\mu^2F^2 - m^2g^2}}{m}. \tag{12}$$

TABLE I

PARAMETERS USED IN THE CALCULATIONS OF TASK TIME WITH AND WITHOUT STIFFNESS ANISOTROPY.

Param.	Value	Param.	Value	Param.	Value
μ	0.6	F	0.2507 N	m	0.0271 kg
g	9.8 m/s^2	f_1+f_2	0.122 N	M	0.3544 kg
S	1.8	B	0.0088 m	b	0.030 m
θ	0.157	y	0.1 m	x	0∼0.6 m

Finally, by substituting Eqs. 10 and 12 into Eq. 1c, the total task time t_a required to complete the pick-and-place motion with stiffness anisotropy can be determined as follows:

$$\begin{aligned} t_a &= 4\sqrt{\frac{y}{a_{a,p}}}+2\sqrt{\frac{x}{a_{a,m}}} \\ &= 2\sqrt{\frac{4my+\mu M\theta^2(B+b)}{2\mu F-mg}}+2\sqrt{\frac{mx}{\sqrt{4\mu^2F^2-m^2g^2}}}. \end{aligned} \tag{13}$$

D. Theoretical Comparison with/without using Stiffness Anisotropy

By using Eqs. 6 and 13, the total task time required to complete the pick-and-place task for both scenarios—with and without stiffness anisotropy—can be calculated. To compare the differences, the parameters listed in Table I were used to compute task times for various translation distances, ranging from $x = 0 \sim 0.6$ m. These parameters are based on actual experimental conditions, which are introduced in the next section.

The calculated task times as a function of translation distance are plotted in Fig. 8 for comparison. The intersection of the two curves appears at a translation distance of approximately $x = 0.018$ m, indicating that the handling operation with stiffness anisotropy (triangle marked curve) outperforms the operation without stiffness anisotropy (circle marked curve) when the translation distance exceeds 0.018 m. Since 0.018 m is a very short distance for most industrial pick-and-place tasks, we can conclude that utilizing stiffness anisotropy significantly enhances handling performance in terms of reducing total task time. Fig. 8 also shows that the difference in task time between the two curves increases with translation distance. At $x = 0.4$ m, the task times for both scenarios are $t_a = 2.43$s (with stiffness anisotropy) and $t_n = 5.28$ s (without stiffness anisotropy), demonstrating that more than half of the total task time can be saved. The maximum allowable accelerations for both scenarios are listed in Table II, where a substantial difference in acceleration can also be observed.

IV. EXPERIMENTS

A. Experimental Validations of Theoretical Analysis

To validate the theoretical findings, experiments were conducted on a pick-and-place task using a 3D-printed box-shaped object. An industrial robotic manipulator (Melfa RV-4FRLD, Mitsubishi Electric Corp.) was used to execute the pick-and-place motions. The object had a mass of 27 g, as listed in Table I. The accelerations provided in Table II were

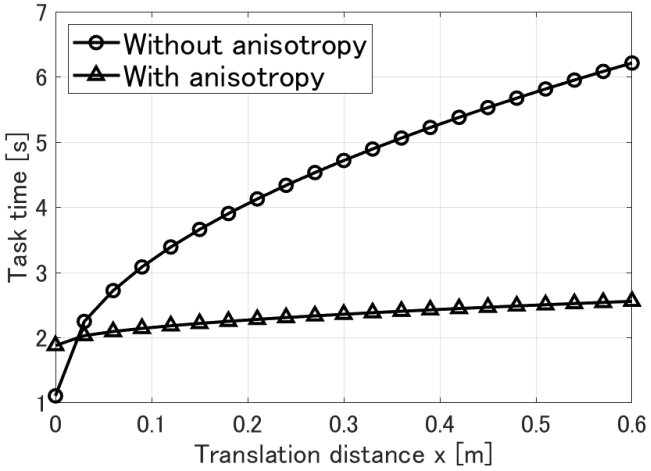

Fig. 8. Theoretical comparison of task times with and without stiffness anisotropy.

TABLE II

THE CALCULATED MAXIMUM ACCELERATIONS AND ANGULAR VELOCITY FOR THE SCENARIOS WITH AND WITHOUT STIFFNESS ANISOTROPY.

Scenario	Motion	Variable	Calculated value
Without anisotropy	Pick up	$a_{n,p}$	1.3011 m/s^2
	Translation	$a_{n,m}$	0.0921 m/s^2
With anisotropy	Pick up	$a_{a,p}$	0.4524 m/s^2
	Translation	$a_{a,m}$	5.2148 m/s^2
	Rotation	ω	1.6697 rad/s

programmed to control the robotic manipulator. A translation distance of $x = 0.4$ m was used in the experiment.

For both scenarios—with and without stiffness anisotropy—experimental snapshots are shown in Figs. 9 and Fig. 10, respectively. Corresponding experimental videos (s1 and s2) are available in the supplementary material. In both cases, the gripper successfully handled the object. The measured accelerations and angular velocities are presented in Table III, showing values comparable to the theoretical predictions.

The measured task times were $t_n = 6.40$ s (without stiffness anisotropy) and $t_a = 3.66$ s (with stiffness anisotropy). Both scenarios required approximately 1.2 s longer than the theoretical predictions. This discrepancy is primarily due to robot arm shaking, which required approximately 0.6 s to stabilize transitions between different motion phases. Overall, the experimental results validate the theoretical analysis and demonstrate the effectiveness of stiffness anisotropy in improving pick-and-place performance.

On the other hand, experiments without stiffness anisotropy were conducted using the translation acceleration from the anisotropy scenario, *i.e.* $a_{a,m} = 5.2148$ m/s^2, which is significantly higher than the allowable acceleration of $a_{n,m} = 0.0921$ m/s^2. Experimental snapshots are shown in Fig. 11, and the corresponding video (s3) is available in the supplementary material. During the translation motion,

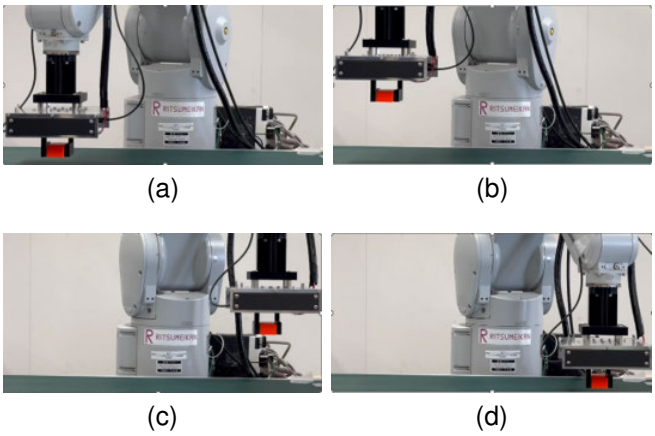

Fig. 9. Experimental snapshots for the scenario without stiffness anisotropy: (a) object grasped, (b) object lifted, (c) object translated to the position above the placement point, and (d) object placed.

TABLE III

MEASURED ACCELERATIONS AND ANGULAR VELOCITY FOR SCENARIOS WITH AND WITHOUT STIFFNESS ANISOTROPY.

Scenario	Motion	Variable	Measured value
Without anisotropy	Pick up	$a_{n,p}$	$1.78\,\mathrm{m/s^2}$
	Translation	$a_{n,m}$	$0.10\,\mathrm{m/s^2}$
With anisotropy	Pick up	$a_{a,p}$	$0.832\,\mathrm{m/s^2}$
	Translation	$a_{a,m}$	$6.16\,\mathrm{m/s^2}$
	Rotation	ω	$1.74\,\mathrm{rad/s}$

the object was dropped, further validating the theoretical analysis and highlighting the necessity of stiffness anisotropy for high-speed handling.

B. Handling Tests on Fragile Objects

Handling tests were conducted to evaluate the gripper's ability to manipulate fragile food items at high speeds. The tested food items included a potato chip, a block of tofu, and a piece of dry seaweed. The physical and motion parameters are provided in Table IV. The motion parameters for the potato chip and tofu were determined based on the theoretical analysis.

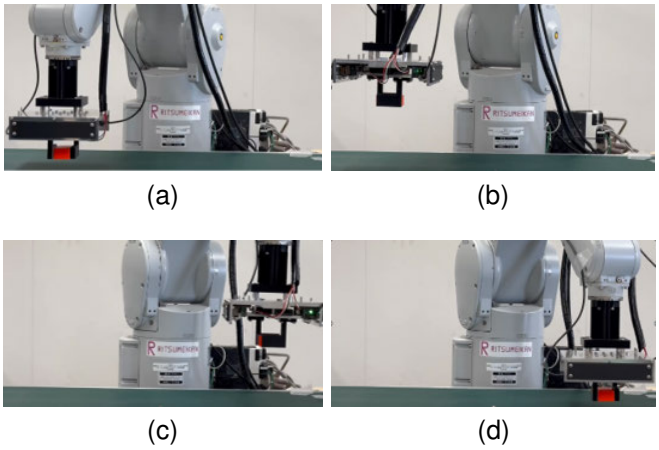

Fig. 10. Experimental snapshots for the scenario with stiffness anisotropy: (a) object grasped, (b) object lifted, (c) object translated to the position above the placement point, and (d) object placed.

Fig. 11. Experimental snapshots for the scenario without stiffness anisotropy but under the high translation acceleration of $a_{a,m} = 5.2148\,\mathrm{m/s^2}$: (a) gripper began translating the object, and (b) object was dropped.

TABLE IV

PHYSICAL OF THE TESTED FRAGILE FOODS AND MOTION PARAMETERS FOR THE HANDLING TESTS.

Food	Mass m	Width b	Force	Motion parameter
Potato chip	1.5 g	50 mm	0.076 N	$a_{a,p} = 0.693\,\mathrm{m/s^2}$
				$a_{a,m} = 23.4\,\mathrm{m/s^2}$
				$\omega = 2.07\,\mathrm{rad/s}$
Tofu	24.0 g	20 mm	0.54 N	$a_{a,p} = 0.949\,\mathrm{m/s^2}$
				$a_{a,m} = 5.60\,\mathrm{m/s^2}$
				$\omega = 2.35\,\mathrm{rad/s}$
Seaweed	0.4 g	33 mm	0.076 N	$a_{a,p} = 0.949\,\mathrm{m/s^2}$
				$a_{a,m} = 5.60\,\mathrm{m/s^2}$
				$\omega = 2.35\,\mathrm{rad/s}$

To enhance grasping stability, a soft silicone material (Ecoflex 00-20, Smooth-On, Inc.) was attached as a cushioning layer on the gripper's finger surfaces when handling the potato chip and seaweed. For handling tofu, a Hyper V sheet material [29] was attached on the finger surfaces to increase the friction coefficient, enabling secure grasping of the wet tofu. The friction coefficient was set to 0.25 for calculating the allowable maximum accelerations and angular velocities, as listed in the fifth column of Table IV.

The grasping forces were set to the minimum force that the gripper could generate for the potato chip and seaweed, while a force of approximately 0.54 N was applied for handling tofu to prevent damage. The calculated maximum accelerations and angular velocities for the potato chip and tofu were implemented in the handling experiments. However, for seaweed, the calculated accelerations were excessively high due to its low weight, exceeding the robotic manipulator's maximum achievable acceleration. Therefore, the same motion parameters as those used for tofu were applied for handling seaweed, as listed in Table IV. Higher accelerations were also attempted in the experiments, but the seaweed was consistently dropped during translation caused by air resistance. This suggests that air resistance significantly affects the stability of seaweed handling due to its extremely low weight, deformability, and thin geometry.

Experimental snapshots with using stiffness anisotropy are shown in Fig. 12. Corresponding experimental videos (s4, s5, and s6) are available in the supplementary material. The robotic gripper successfully handled all three fragile food items under the calculated allowable accelerations listed in Table IV. Conversely, when the same accelerations were applied in handling tests without using stiffness anisotropy, the gripper failed to handle all three food items, as observed in the experimental snapshots shown in Fig. 13. Corresponding

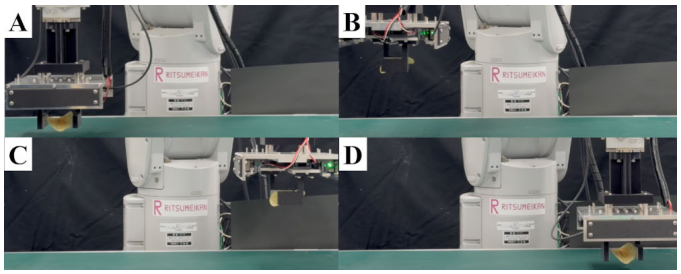

(a) Handling test on a potato chip

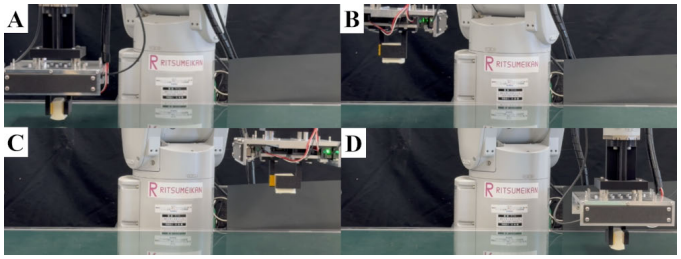

(b) Handling test on a block of tofu

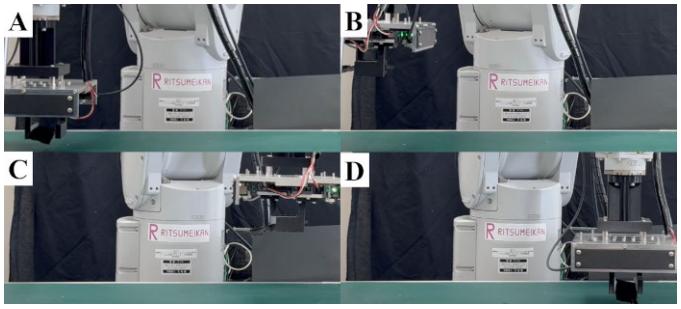

(c) Handling test on a piece of seaweed

Fig. 12. Experimental snapshots of handling different fragile food items with stiffness anisotropy. A, B, C, and D denote the different end moments of grasping, lifting, translating, and placing, respectively.

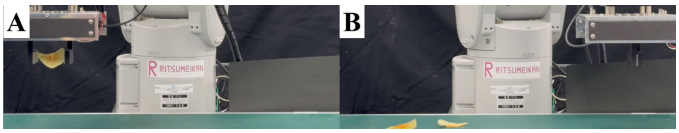

(a) Handling test on a potato chip

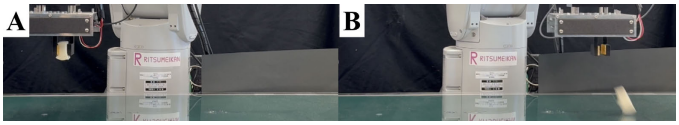

(b) Handling test on a block of tofu

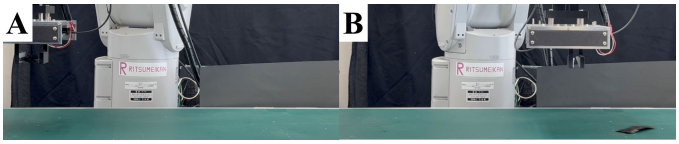

(c) Handling test on a piece of seaweed

Fig. 13. Experimental snapshots of handling different fragile food items without stiffness anisotropy. A and B denote the different end moments of lifting and translating, respectively.

experimental videos (s7, s8, and s9) are also available in the supplementary material.

These results indicate that the proposed gripper can effectively grasp fragile objects without causing damage, owing to the minimal grasping forces that the gripper can generate. Furthermore, the gripper enables high-speed pick-and-place handling of fragile food items, such as the potato chip, tofu, and dry seaweed, when utilizing the stiffness anisotropy strategy. In contrast, without utilizing the stiffness anisotropy, the gripper is unable to achieve successful handling of these fragile foods at the same high speeds. The handling failures happened during acceleration for potato chip due to collapse and deceleration for tofu and seaweed due to dropping.

V. Conclusions

In this paper, we presented a robotic gripper driven by two linear motors. It can generate a grasping force as small as approximately 0.076 N without relying on external force sensors. The gripper exhibits high compliance (low stiffness) in the grasping direction, allowing its fingers to back-drive at a force of approximately 0.122 N, thereby preventing damage to fragile food items. Conversely, in the direction perpendicular to grasping, the gripper demonstrates extremely high stiffness due to its rigid structure. Consequently, the gripper achieves extreme stiffness anisotropy.

To leverage stiffness anisotropy, this paper analyzed the maximum allowable accelerations for a typical pick-and-place handling operation with and without using stiffness anisotropy. The analysis indicated that handling strategy with using stiffness anisotropy outperforms handling strategy without using it, provided the translation distance exceeds a minimal threshold of 0.018 m. By utilizing stiffness anisotropy, total task time can be reduced by more than half.

Experiments were conducted using a 3D-printed object, and the results aligned with the theoretical analysis. Without stiffness anisotropy, high-speed motion could not be achieved, whereas implementing stiffness anisotropy reduced the actual task time by approximately 43%. Additionally, high-speed handling tests were conducted on three fragile food items: a potato chip, a block of tofu, and a piece of dry seaweed. The maximum accelerations were set to 23.4 m/s^2 for the potato chip and 5.6 m/s^2 for both tofu and seaweed. Results demonstrated that handling tests with stiffness anisotropy were successful, whereas all three food items were dropped during translation when stiffness anisotropy was not used. These findings clearly highlight the advantages of the proposed robotic gripper in handling fragile foods, leveraging its extreme stiffness anisotropy.

Future work will explore position control of the fingers and the execution of in-hand manipulation tasks using the proposed robotic gripper.

References

[1] P. Y. Chua, T. Ilschner, and D. G. Caldwell, Robotic manipulation of food products - a review, Industrial Robot, vol. 30, no. 4, pp. 345–354, Aug. 2003.

[2] T. R. C. Konfo, F. M. C. Djouhou, M. H. Hounhouigan, et al., Recent advances in the use of digital technologies in agri-food processing: A short review, Applied Food Research, vol. 3, no. 2, 100329, 2023.

[3] R. Badia-Melis, U. M. Carthy, L. Ruiz-Garcia, et al., New trends in cold chain monitoring applications - a review, Food Control, vol. 86, pp. 170–182, Apr. 2018.

[4] Z. Wang, S. Hirai, and S. Kawamura, Challenges and opportunities in robotic food handling: A review, Frontiers in Robotics and AI, vol. 8, no. 789107, Jan. 2022.

[5] J. Lee, R. Sun, A. Bylard, et al., Grasp Failure Constraints for Fast and Reliable Pick-and-Place Using Multi-Suction-Cup Grippers, 2024. [Online]. Available: https://arxiv.org/abs/2408.03498.

[6] D. Liu, M. Wang, N. Fang, et al., Design and tests of a non-contact Bernoulli gripper for rough-surfaced and fragile objects gripping, Assembly Automation, vol. 40, no. 5, pp. 735–743, Sept.2020.

[7] R. Mykhailyshyn and A. M. Fey, Low-Contact Grasping of Soft Tissue with Complex Geometry using a Vortex Gripper, 2025. [Online]. Available: https://arxiv.org/abs/2501.07832.

[8] J. H. Low, P. M. Khin, Q. Q. Han, et al., Sensorized reconfigurable soft robotic gripper system for automated food handling, IEEE/ASME Transactions on Mechatronics, vol. 27, no. 5, pp. 3232–3243, Oct. 2022.

[9] Y. Liu, J. Zhang, Y. Lou, et al., Soft bionic gripper with tactile sensing and slip detection for damage-free grasping of fragile fruits and vegetables, Computers and Electronics in Agriculture, vol. 220, no. 108904, pp. 1–13, Apr. 2024.

[10] H. Huang, S. Tang, W. Chai, et al., Mcsg: A morphology configurable soft gripper with self-adaption modular composite finger, IEEE Transactions on Industrial Electronics, vol. 71, no. 1, pp. 708–717, Jan. 2024.

[11] H. Enomoto, M. Ishige, T. Umedachi, et al., Delicate jamming grasp: Detecting deformation of fragile objects using permanent magnet elastomer membrane, IEEE Robotics and Automation Letters, vol. 9, no. 2, pp. 979–986, Feb. 2024.

[12] S. T. Bui, S. Kawano, and V. A. Ho, Rose: Rotation-based squeezing robotic gripper toward universal handling of objects, in Robotics: Science and Systems, pp. 1–10, Jul. 2023.

[13] Y. Hao, Z. Wang, Y. Zhou, et al., A soft enveloping gripper with enhanced grasping ability via morphological adaptability, Advanced Intelligent Systems, no. 2200456, Apr. 2023.

[14] J. Lee, Y. Seo, C. Park, et al., Shape-adaptive universal soft parallel gripper for delicate grasping using a stiffness-variable composite structure, IEEE Transactions on Industrial Electronics, vol. 68, no. 12, pp. 12441–12451, Dec. 2021.

[15] R. Maruyama, T. Watanabe, and M. Uchida, Delicate grasping by robotic gripper with incompressible fluid-based deformable fingertips, in 2013 IEEE/RSJ International Conference on Intelligent Robots and Systems (IROS), pp. 5469–5474, Nov. 2013.

[16] B. An, T. Choi, and U. Kim, Linkage integrated fin ray gripper capable of safe adaptive grasping for tomato harvesting, Computers and Electronics in Agriculture, vol. 232, no. 110118, Feb. 2025.

[17] Y. Zhang, Z. Wang, K. Kutani, et al., A soft-containing gripper for high-speed handling of breadcrumb-coated oysters, Journal of Field Robotics, vol. 24, no. 5, pp. 1976-1990, Dec. 2024.

[18] Y. Piskarev, A. Devincenti, V. Ramachandran, et al., A soft gripper with granular jamming and electroadhesive properties, Advanced Intelligent Systems, vol. 5, no. 2200409, Mar. 2023.

[19] M. Zhu, Y. Mori, T. Wakayama, et al., A fully multi-material three-dimensional printed soft gripper with variable stiffness for robust grasping, Soft Robotics, vol. 6, no. 4, pp. 507–519, Aug. 2019.

[20] J. Amend, N. Cheng, S. Fakhouri, et al., Soft Robotics Commercialization: Jamming Grippers from Research to Product, Soft Robotics, vol. 3, no. 4, pp. 213–222, Dec. 2016.

[21] Z. Wang, R. Kanegae, and S. Hirai, Circular shell gripper for handling food products, Soft Robotics, vol. 8, no. 5, pp. 542–554, Oct. 2021.

[22] L. Gerez, C.-M. Chang, and M. Liarokapis, Employing Pneumatic, Telescopic Actuators for the Development of Soft and Hybrid Robotic Grippers, Frontiers in Robotics and AI, vol. 7, no. 601274, Nov. 2020.

[23] Z. Wang, H. Furuta, S. Hirai, et al., A scooping-binding robotic gripper for handling various food products, Frontiers in Robotics and AI, vol. 8, no. 640805, Mar. 2021.

[24] P. V. Nguyen, D. B. Sunil, and W. T. Chow, Soft-stable interface in grasping multiple objects by wiring-tension, Scientific Reports, vol. 13, no. 21537, Dec. 2023.

[25] S. Yang, Y. Zhou, I. D. Walker, et al., Dynamic capture using a trap-like soft gripper with stiffness anisotropy, IEEE/ASME Transactions on Mechatronics, vol. 28, no. 3, pp. 1337–1346, Jun. 2023.

[26] P. van Assenbergh, C. Culmone, P. Breedveld, et al., Implementation of anisotropic soft pads in a surgical gripper for secure and gentle grip on vulnerable tissues, Journal of Engineering in Medicine, vol. 235, no. 3, pp. 255–263, Mar. 2021.

[27] R. Mykhailyshyn, J. Lee, M. Mykhailyshyn, K. Harada, and A. M. Fey, Dexterous Manipulation of Deformable Objects via Pneumatic Gripping: Lifting by One End, 2025. [Online]. Available: https://arXiv:2501.05198v1.

[28] M. Sato, H. Arita, Y. Mori, et al., A sensorless parallel gripper capable of generating sub-newton level grasping force, in The 2024 16th IEEE/SICE International Symposium on System Integration (SII 2024), Jan. 2024.

[29] Z. Wang, T. Hirata, T. Sato, et al., A soft robotic hand based on bellows actuators for dishwashing automation, IEEE Robotics and Automation Letters, vol. 6, no. 2, pp. 2139–2146, Feb. 2021.